Maternal Thyroid Hormones Are Essential for Neural Development in Zebrafish

Marco A. Campinho, João Saraiva, Claudia Florindo, and Deborah M. Power

Comparative Endocrinology and Integrative Biology Group (M.A.C., J.S., D.M.P.), Centre of Marine Sciences, and Departamento de Ciências Biomédicas e Medicina and Centro de Biomedicina Molecular e Estrutural (C.F.), Universidade do Algarve, 8005-139 Faro, Portugal

Teleost eggs contain an abundant store of maternal thyroid hormones (THs), and early in zebrafish embryonic development, all the genes necessary for TH signaling are expressed. Nonetheless the function of THs in embryonic development remains elusive. To test the hypothesis that THs are fundamental for zebrafish embryonic development, an monocarboxilic transporter 8 (Mct8) knockdown strategy was deployed to prevent maternal TH uptake. Absence of maternal THs did not affect early specification of the neural epithelia but profoundly modified later dorsal specification of the brain and spinal cord as well as specific neuron differentiation. Maternal THs acted upstream of *pax2a*, *pax7*, and *pax8* genes but downstream of *shha* and *fgf8a* signaling. The lack of inhibitory spinal cord interneurons and increased motoneurons in the *mct8* morphants is consistent with their stiff axial body and impaired mobility. The *mct8* mutations are associated with X-linked mental retardation in humans, and the cellular and molecular consequences of MCT8 knockdown during embryonic development in zebrafish provides new insight into the potential role of THs in this condition. **(*Molecular Endocrinology* 28: 1136–1149, 2014)**

Thyroid hormones (THs) constitute key signaling molecules that regulate vertebrate development and physiology. Given the capacity of these hormones to regulate and/or influence a wide range of molecular pathways, their availability, intracellular transport, and metabolism are tightly regulated. This is especially evident in the brain where the prohormone T_4 is transported to neural auxiliary cells via the blood-brain barrier (BBB), is converted to the active hormone T_3 and then actively transported into neurons and other target cells (1–7). In chickens and mammals, maternal THs are essential for the development of the brain and other organs (8–17). Elements of the thyroid cellular signaling pathway are detected in developing rodent brain (10) and T_3 interacts with TH receptors (TRs) to transactivate or repress gene expression (10, 12, 13, 18, 19).

Teleost fish embryonic development is dependent on nutrients, hormones, and maternal mRNA laid down during egg maturation. Fish eggs contain a substantial concentration of maternal THs that are gradually depleted as the embryo develops (20–22). Although TRs (*thraa*, *thrab*, and *thrb*) have been identified in developing teleost embryos, the function of maternal THs is uncertain (21, 23–28). Functional studies of TRs during early teleost development in zebrafish suggest they have a ligand-independent function and repress retinoic acid signaling (24, 25). The recent identification of the TH-specific membrane transporter monocarboxylic transporter 8 (*mct8*) during zebrafish embryonic development and its functional characterization as an TH transporter ($T_3 \gg T_4$) (29) suggests maternal THs have a functional role. An *mct8* promoter-driven transgenic zebrafish line revealed *mct8* is primarily expressed in the nervous and vascular systems and conditional MCT8 knockdown severely disrupted brain development (30), but the genetic networks and functional basis of the defects are not established. We hypothesized that the *mct8* phenotype reveals that maternal THs accumulated in the egg are essential in teleost fish

ISSN Print 0888-8809 ISSN Online 1944-9917
Printed in U.S.A.

Received January 26, 2014. Accepted May 14, 2014.
First Published Online May 30, 2014

Abbreviations: BBB, blood-brain barrier; CTRMO, control MO; hpf, hours post fertilization; MCT8, monocarboxylic transporter 8; MHB, midbrain-hindbrain boundary; MO, morpholino; PBT, PBS/Tween 20; PFA, paraformaldehyde; TH, thyroid hormone; TR, TH receptor; TUNEL, terminal deoxynucleotidyl transferase dUTP nick end labeling; WISH, whole-mount in situ hybridization.

embryogenesis. In the present study, we used an MCT8 knockdown strategy as a means by which to prevent maternal TH uptake by the developing embryo up to 48 hours after fertilization before the system for TH production is established (31, 32). This strategy provides a unique opportunity to study the function of maternal THs during early brain and spinal cord development in zebrafish.

The aim of the present study is to test the hypothesis that the neurological defects in Mct8 knockdown zebrafish reveal the effect of disrupting TH driven embryonic events. The importance of THs for the formation of interneurons in the hindbrain and for specification of different neuronal spinal cord lineages in zebrafish embryos is revealed using an Mct8 knockdown strategy to block maternal TH uptake. The results reveal that maternal THs play an essential role in the developing zebrafish brain and that *mct8* has a key role as it regulates cellular TH availability. Furthermore, the evidence strongly suggests that *mct8* and THs are key factors regulating the coordination between the development of the zebrafish brain and its vascularization. The results highlight the potential of this zebrafish experimental model to understand at the cellular and molecular level X-linked mental retardation associated in humans with MCT8 mutations.

Materials and Methods

Animal husbandry and wild-type embryo collection

Zebrafish AB strain adults were kept in a recirculating system (Techniplast) at 28°C, under a 14-hour light, 10-hour dark cycle and fed twice daily with dry pellets (Aquatic Nature) and once with enriched *Artemia nauplii*. Natural spawning was promoted (33) by placing adult couples in a mating box (Techniplast) separated by a Perspex screen overnight and then removing it at the start of the light phase the following day. Fertilized eggs were collected into standard zebrafish E3 medium (5mM NaCl, 0.17mM KCl, 0.33mM CaCl, 0.33mM $MgSO_4$) and reared at 28.5°C in an incubator (Sanyo) under a 12-hour, 12-hour dark cycle. Staging was done according to Kimmel et al (33) after observation for developmental landmarks.

Wild-type embryos for cloning and generation of riboprobes or for determination of the expression pattern of zebrafish *mct8*, *thraa*, *thrab*, and *thrb* were sampled at 12, 24, 31, 48, and 72 hours post fertilization (hpf). Embryos were manually dechorionated and either snap-frozen and stored in liquid nitrogen or fixed overnight at 4°C in 4% paraformaldehyde (PFA)/1× PBS. After 4% PFA fixation, animals were washed twice for 5 minutes in 1× PBS/0.1% Tween 20 (1× PBT) and transferred to methanol, through a graded series (25%–100% methanol) diluted with 1× PBT and kept at −20°C until use. When necessary, animals were depigmented before storage in methanol (100%) (34).

Table 2. Sequences of MOs Used

MO	Sequence
MCT8MO	TCATCGCTTTCCGAGTGCATCCTAC
CTRMO	CCTCTTACCTCAGTTACAATTTATA

Whole-mount in situ hybridization

Zebrafish *pax8* (XM_001339857.2), *shha* (NM_131063.2), and *thrb* (NM_131340.1) riboprobes were generated by PCR amplification and cloning. cDNA synthesis was carried out with 500 ng of DNA-free zebrafish embryo total RNA, extracted with the OMEGA total RNA extraction kit, and 5 ng/μL random hexamers using a Promega Moloney Murine Leukemia Virus first-strand cDNA kit. Primers (Table 1) were designed for the target templates using sequences retrieved from National Center for Biotechnology Information. PCRs were performed using zebrafish cDNA (200 ng/μL); DreamTaq 1× buffer (Fermentas); 2mM $MgCl_2$, 0.2mM dNTPs, and 0.2μM zebrafish specific primers for *pax8*, *shha*, and *thrb* (Table 1); and 0.03 U/μL DreamTaq polymerase (Fermentas). The PCR cycle was carried out using a BioRad MyCycler as follows: 5 minutes at 95°C, 35 cycles of 30 seconds at 95°C, 30 seconds at the appropriate primer annealing temperature (see Table 1), and 1.5 minutes at 72°C followed by a final 5-minute step at 72°C. PCR products were agarose gel purified using a GFX gel band extraction kit (GE Healthcare), suspended in water, and cloned into pGemT-easy vector (Promega). Isolated bacterial colony plasmid DNA was extracted and sequenced to confirm identity and orientation of the zebrafish *pax8*, *shha*, and *thrb* sequences.

The plasmids for zebrafish *fgf8a* (NM_131281.2) was a kind gift from Dr Lisa Maves, *thraa* (NM_131396.1) and *thrab* (XM_001920978.4) were kindly provided by Dr Sachiko Takayama, and *pax2a* (NM_130934.1) was kindly provided by Dr Fumihito Ono. The plasmid with zebrafish *mct8* (JQ966310) was a kind gift from the Singapore Genome Institute.

Ten nanograms of plasmid DNA for zebrafish *mct8*, *pax8*, *shha*, *thrb*, *fgf8*, and *thraa* were used to PCR amplify the template and the T7 and SP6 RNA polymerase promoter in the

Table 1. Primers Used for PCR Cloning and Mutagenesis

Gene	Forward Primer	Reverse Primer
pax8	ACAACGGCGAACACCAACACC	TTAGAGATGATCATAGGCAGC
shha	CAGCGTGCGGCAAAATGCGGC	CACGAGGGTTTTCAGCTTGAG
mct8	ATGCACTCGGAAAGCGATGA	TCATATGTGTGTCTCCATGTC
thrb	GGCCTAATATACTGCAGTATGTC	ACAGGGAGACTGTAGAGGTCTGAC
mut*mct8*[a]	GTAGGATGCA[underln]TAGCGAGAGCGACGACAACAC	TCATATGTGTGTCTCCATGTC

[a] In the mut*mct8* forward primer, the underlined sequence indicates the bases substituted.

flanking multiple cloning site. The PCR conditions were identical to the conditions described above with the exception that universal M13 forward and reverse primers were used, and the annealing temperature was 60°C. PCR products were agarose gel purified and extracted using a GFX gel band extraction kit according to the manufacturer's instruction (GE Health). For the zebrafish *thrab* clone, 5 μg plasmid DNA was digested with Fermentas fast digest *Spe*I, agarose gel purified, and extracted using a GFX gel extraction kit according to the manufacturer's instructions.

Whole-mount in situ hybridization (WISH) cRNA probes complementary to zebrafish were in vitro transcribed and labeled with DIG (Roche). Probes for *fgf8*, *thrb*, and *thrab* were produced with T7 RNA polymerase (Fermentas), whereas *pax8*, *thraa*, *shha*, and *mct8* probes were produced in vitro with SP6 RNA polymerase (Fermentas) according to the manufacturer's instructions. WISH was performed as described previously (34) using 0.25 ng/μL probe at a hybridization temperature of 70°C. Animals were transferred to 100% glycerol and imaged using an Olympus SZX7 stereoscope coupled to an Optikam 3.0 digital camera.

mct8 knockdown

A translation blocking morpholino (MO) was designed against the zebrafish *mct8* genomic sequence and acquired from Gene Tools, LLC. The MCT8MO was diluted to 2mM in 1× MO buffer (5mM HEPES [pH 7.5] and 200mM KCl) and kept at −20°C until use. A preliminary study was carried out, and 1 nL of the MO stock diluted to 0.4mM (n = 135), 0.6mM (n = 117), and 0.8mM (n = 95) in 1× MO buffer was microinjected into 1- to 4-cell stage wild-type embryos collected as described above. Noninjected embryos (n = 94) and embryos microinjected at the 1- to 4-cell stage with 1 nL 0.6mM control MO (CTRMO) (n = 127; Gene Tools) were used as controls. A fully penetrant phenotype was observed only in 0.8 pmol MCT8MO-microinjected animals, and that concentration was selected for all subsequent experiments.

Nonspecific MCT8MO effects were determined using wild-type embryos at the 1- to 4-cell stage collected as previously described and microinjected (1 nL in any experimental group) with 0.8 pmol MCT8MO (n = 342), 0.8 pmol MCT8MO plus 0.5 pmol p53MO (35) (n = 351), or CTRMO (n = 280) (Gene Tools). In parallel, noninjected embryos were also taken from each batch of embryos used (n = 352). Animals were incubated at 28.5°C and fixed at 25 hpf in 4% PFA/1× PBS (pH 7.4) as described above (33). Embryos were rehydrated to 1× PBT and washed for 15 minutes at room temperature in 1× PBS/0.1% Triton X-100 (Sigma)/0.1M sodium acetate (pH 6). Embryos were further treated for 15 minutes at room temperature with 1 μg/mL Proteinase K (Sigma) followed by four 5-minute washes in 1× PBT. Apoptotic cells in experimental animals (n = 20) were identified using the Roche in situ cell death TMR-red detection kit according to the manufacturer's instructions. Animals were photographed using a Leica DM2000 light fluorescent microscope coupled to a Leica DFC480 digital camera. For the positive control, 5 animals per experimental group were taken and treated for 30 minutes with RQ deoxyribonuclease I (40 U/μL; Promega) at 37°C. For the negative control, 5 animals per experimental group went through the same procedure, but the enzyme mix solution (Roche) was omitted. Individual animals from each experimental group were transferred to black flat-bottom 96-well Fluotrac600 plates (Greiner Bio-One) in 100 μL 1× PBS (n = 12). Total fluorescence was measured by excitation in the visible spectrum and quantification of fluorescent emission at 570 nm in a BioTek Synergy HT multimode microplate reader. Background emission was determined by scanning 12 microplate wells containing 100 μL 1× PBS only. Total fluorescence of individual experimental animals was calculated (absolute fluorescent value − mean absolute fluorescence of wells containing 1× PBS). Statistical analysis was performed using the Prism version 4 software. Statistically significant differences between experimental groups were determined using one-way ANOVA followed by Bonferroni multiple-comparison post hoc analysis using the Prism version 4 software. Statistical significance was considered at $P < .05$.

Rescue experiments to determine MCT8MO specificity was carried out by microinjecting (1 nL) transgenic *Tg*(*fli1*:*GFP*) (36) embryos in the 1- to 4-cell stage with either 0.8 pmol MCT8MO (n = 105) or 100 pg zebrafish *mct8* mRNA (n = 132) or coinjecting 0.8 pmol MCT8MO with 100 pg zebrafish *mct8* mRNA (n = 106). As controls, embryos were either noninjected (n = 129) or injected with CTRMO (n = 123) (Gene Tools). For *mct8* mRNA production, the entire coding cDNA region (Table 1) was amplified by PCR as described above using a forward primer that introduced 6 silent mutations in the 5′-seeding region (wild-type sequence: GTAGGATGCACTCGGAAAGCGATGA; mutated sequence: GTAGGATGCATAGCGAGAGCGACGA) of the MCT8MO. (The underlined nucleotides indicate the mutated positions.) The amplified fragment was gel purified as described above and cloned into pCS2+ plasmid. Five micrograms of pCS2+ *mct8*-mut were linearized with *Not*I (Thermo Scientific), gel purified, and diluted in water. The 5 μg of linearized pCS2+ *mct8*-mut plasmid was used as the template for in vitro translation of zebrafish *mct8* mutated mRNA using an mRNA Messenger Machine kit (Ambion) and following the manufacturer's instructions. Before preparation for microinjection, mRNA was purified in phenol/chloroform, diluted in ribonuclease-free water and frozen at −80°C until use. Experimental live embryos were manually dechorionated if necessary and anesthetized with 0.001% MS222 in E3 medium. Development of the brain vasculature in experimental embryos was observed (n = 20 per group) by live imaging at 48 hpf using a Leica DM2000 fluorescent microscope coupled to a Leica DFC480 camera. Terminal deoxynucleotidyl transferase dUTP nick end labeling (TUNEL) apoptosis analysis was performed as described above.

After validation of the MCT8MO, final experiments were performed to characterize the MCT8 knockdown phenotype using 3 different egg batches of wild-type zebrafish. In parallel, embryos were microinjected at the 1- to 4-cell stage with 1 nL of either CTRMO (0.6 pmol; n = 263) or MCT8MO (0.8 pmol; n = 320). Developing embryos were sampled at 25, 31, and 48 hpf.

Fluorescent immunohistochemistry

Embryos (n = 20 per experimental group) were hydrated through a graded series of methanol (100%–0%)/1× PBT (Sigma-Aldrich), followed by 4 × 5 minutes in PBTr (1× PBS + 0.1% Triton X-100) and preincubated in 1× PBT/10% sheep serum at room temperature for 2 hours. Embryos were then incubated overnight at 4°C in preincubation solution with 1/25 anti-Pax7 serum (Developmental Studies Hybridoma Bank) and washed, and secondary goat antimouse IgG H+L conjugated

with Hilyte-596 (1/400; Anaspec) was used for detection. To highlight neuronal structures, a mouse antiacetylated β-tubulin (1/1000; Sigma-Aldrich) was used and detected with a goat antimouse IgG2β antibody conjugated to Alexa-488 (Invitrogen). For Zn8 immunohistochemistry, the samples were prepared as described above and incubated with Zn8 (1/20; Developmental Studies Hybridoma Bank) overnight at 4°C in 1× PBS/10% sheep serum/0.5% Triton X-100. Fluorescent detection was carried out using a goat antimouse IgG (H+L) secondary antibody conjugated with HiLyte-488 (1/400; Anaspec).

After staining, samples were transferred to glycerol and fluorescent microscope imaging carried out with a Leica DM2000 fluorescent microscope coupled to a DFC480 digital camera or a Zeiss Z2 fluorescent microscope coupled to a Zeiss HRm digital camera. Images were deconvoluted using SVI Huygens software 4.4 and figures assembled in Photoshop software (Adobe).

Mobility assay

Touch-and-go mobility assays were performed in 72-hpf experimental embryos to understand how MCT8 knockdown would affect neural network formation in the spinal cord. Zebrafish embryos at 72 hpf microinjected (1 nL) with either 0.6 pmol CTRMO (n = 15) or 0.8 pmol MCT8MO (n = 15) were used. Movement of larvae from each experimental group were recorded for 1 minute after they were touched in the posterior trunk with a tungsten needle, and the distance they traveled was recorded using a Sony DV camera. Tracker software (37) was used to measure the distance covered by experimental zebrafish larvae. Statistical analysis on ranks followed by Dunnet's post hoc test was performed to determine significant effects on motility ($P < .05$) using SPSS version 20 software.

Results

TH cellular signaling components are expressed in early zebrafish embryos

The expression of *mct8* is detected in the neural epithelia from 12hpf (Figure 1A and Supplemental Figures 1A and 2) and is most abundant in the optic vesicles and rhombomeres 3 and 5 (arrowheads in Figure 1A). By 24 hpf, *mct8* expression is localized in most of the developing brain but is most abundant in the retina, at the outer edge of the brain ventricle, and along the hindbrain and spinal cord (Figure 1E and Supplemental Figure 1E and 2). The cells lining the otic capsule also have abundant *mct8* expression (white arrows in Figure 1E and Supplemental Figures 1E and 2). A considerable reduction in brain *mct8* expression is evident at 31 hpf (Figure 1I and Supplemental Figures 1I and 2) and mainly located in the outer lining of the first ventricle, the retina, and the midbrain-hindbrain boundary (MHB) (Figure 1I and Supplemental Figures 1I and 2). At 31 hpf, *mct8* expression is significantly decreased in the hindbrain and spinal cord and totally absent from the otic capsule (Figure 1I and Supplemental Figures 1I and 2). By 48 hpf, *mct8* expression is mainly present in the developing BBB (Figure 1M and Supplemental Figures 1M and 2). At the last time point studied, 72 hpf, *mct8* expression is found only in invading blood vessels of the brain and in the BBB (Figure 1Q and Supplemental Figures 1Q and 2).

At 12 hpf, neither *thraa* nor *thrb* are expressed in zebrafish embryos (Figure 1, B and D, and Supplemental Figure 1, B and D). The expression of *thraa* increases significantly in the retina and most of the brain and spinal cord at 24 hpf (Figure 1F and Supplemental Figure 1F) and is most abundant in the developing forebrain, around the first ventricle (Supplemental Figure 1F) and in the hindbrain and spinal cord (Figure 1F). In parallel, *thraa* is expressed in the same cell layer or in an adjacent layer to *mct8* (Figure 1, E and F) in the otic capsule. At 31 hpf, *thraa* continues to be expressed at low lev-

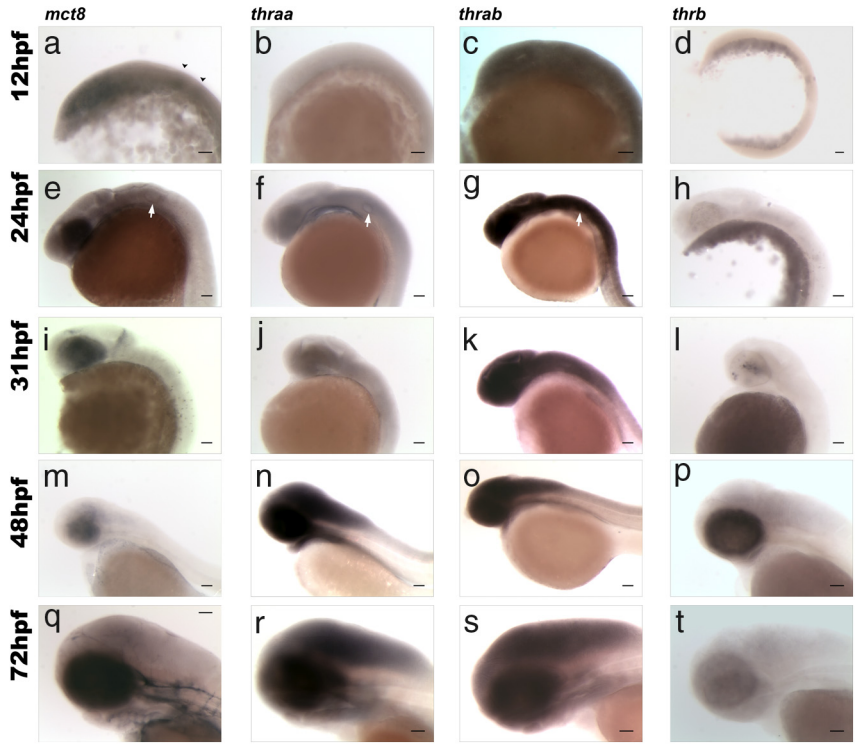

Figure 1. Lateral views of zebrafish embryos at 12 (A–D), 24 (E–H), 31 (I–L), 48 (M–P), and 72 (Q–T) hpf showing results of WISH for expression of *mct8* (A, E, I, M, and Q), *thraa* (B, F, J, N, and R), *thrab* (C, G, K, O, and S), and *thrb* (D, H, L, P, and T). In A, black arrowheads denote rhombomeres 3 and 5. In E, F, and G, white arrows indicate the otic vesicle. Scale bars, 100 μm.

els in the developing brain and spinal cord and is mostly localized in the first ventricle wall lining (Figure 1J and Supplemental Figure 1J). From 48 hpf onward, *thraa* expression is found at much higher levels in most of the brain and spinal cord (Figure 1, N and R, and Supplemental Figure 1, N and R).

Zebrafish *thrab* is highly expressed throughout the neural epithelia in embryos at 12 hpf (Figure 1C and Supplemental Figure 1C). By 24 hpf, it is highly expressed in the entire brain and spinal cord (Figure 1G and Supplemental Figure 1G) and is absent from the otic capsule (white arrowhead in Figure 1G and Supplemental Figure 1G) but is present in the surrounding neural tissue (Supplemental Figure 1G). Expression of *thrab* remains high in the brain and spinal cord at 48 hpf (Figure 1O and Supplemental Figure 1O) and 72 hpf (Figure 1S and Supplemental Figure 1S). At 31 hpf (Figure 1L and Supplemental Figure 1L), *thrb*-positive cells are first evident in the retina and by 48 hpf, *thrb*-positive retina cells increase in number and distribution and low expression is visible in the diencephalon and hindbrain (Figure 1P and Supplemental Figure 1P). Comparison of *thrb* (Figure 1T and Supplemental Figure 1T), *thraa* (Figure 1R and Supplemental Figure 1R), and *thrab* (Figure 1S and Supplemental Figure 1S) at 72 hpf reveals they all have a widespread distribution in the brain. However, *thraa* and *thrab* are expressed in regions adjacent to *mct8*-expressing vessels in the brain and spinal cord (Figure 1Q and Supplemental Figure 1Q). *Thrab* is also found in the primary head sinus where *mct8* is also expressed (Figure 1, Q and 1S). Overall, all the necessary and sufficient factors needed for maternal THs to elicit their function are present early in zebrafish development.

Maternal THs are bona fide signaling molecules in zebrafish development

As a first trial, the MO against MCT8 (MCT8MO) was microinjected (1 nL) at 0.4mM, 0.6mM, and 0.8mM and the embryos left to develop up until 48 hpf. Intact noninjected animals or embryos microinjected (1 nL) with the CTRMO (0.6mM standard CTRMO; Gene Tools) did not differ from the noninjected control animals (Figure 2). The MCT8MO has a notable phenotype only from 0.6 pmol upward and at 0.8 pmol is fully penetrant (Figure 2A). The 0.6- and 0.8-pmol morphants are smaller than the control and 0.4-pmol MCT8MO microinjected siblings and have a pronounced lateral curvature of the axial trunk (Figure 2A), which is randomly distributed between the right and left side.

Brain development is altered in the 0.6- and 0.8-pmol *mct8* morphants (Figure 2B). Cells expressing *pax8*, which labels different neuron populations in the MHB and the hindbrain (38), decreased with increasing concentration of MCT8MO microinjection (Figure 2B). In 0.4-pmol MCT8 morphants, *pax8*-positive cells are somewhat reduced, even though brain morphology seems mostly identical to control animals, but in 0.6-pmol morphants *pax8*-expressing cells are severely reduced in the hindbrain and MHB (arrowheads in Figure 2B) concomitant with severely disrupted brain development (Figure 2B). In 0.8-pmol *mct8* morphants, *pax8*-expressing cells in both the hypothalamus and the hindbrain are absent. Using both the axial body bending phenotype and *pax8* expression in the hindbrain, we concluded that 0.8 pmol MCT8MO is a fully penetrant dose, and all morphants had the same phenotype. This evidence was taken as an indirect qualitative measure of the efficacy of the 0.8-pmol MCT8MO dosage in the absence of specific antisera to quantify MCT8 expression. From this point onward, all experiments were carried out using 0.8 pmol MCT8MO.

At 25 hpf, the 0.8-pmol MCT8MO zebrafish morphants have severe impairment of brain development (Figure 3A). Almost all brain regions are affected, including the eye, and they appear smaller than in control ani-

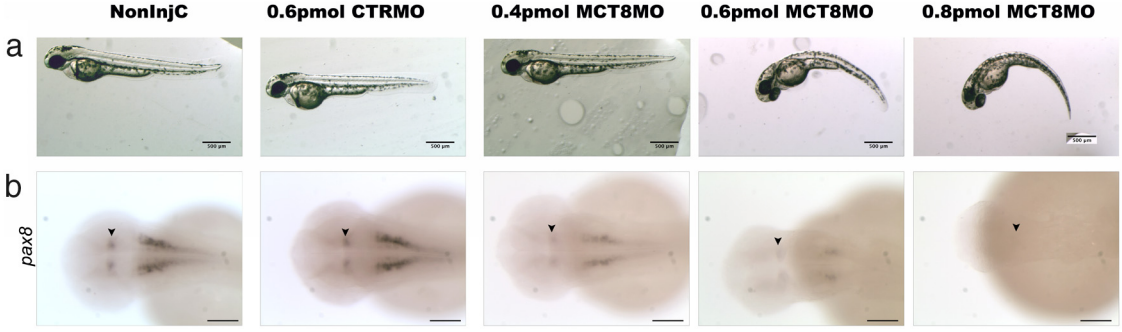

Figure 2. MCT8MO titration. A, Bright-field images of 48-hpf wild-type zebrafish embryos noninjected or microinjected with 0.6 pmol CTRMO or 0.4, 0.6, or 0.8 pmol MCT8MO. Scale bars, 500 μm. B, To further understand the phenotype and penetrance of the MCT8MO, WISH for *pax8* was carried out in 48-hpf wild-type zebrafish embryos noninjected or microinjected with 0.6 pmol CTRMO or 0.4, 0.6, or 0.8 pmol MCT8MO. Scale bars, 100 μm.

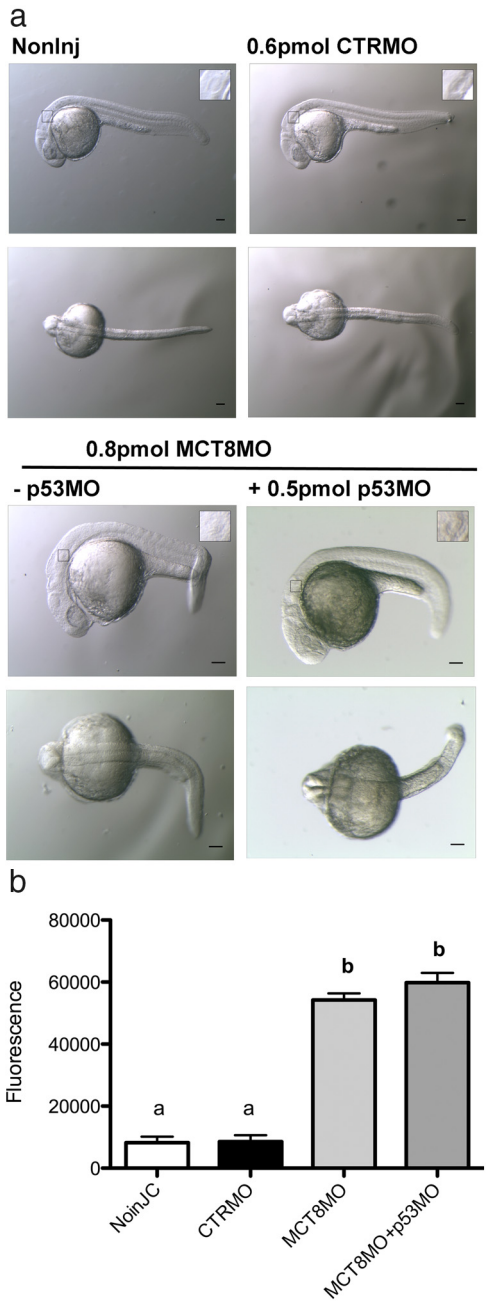

Figure 3. Increased apoptosis in *mct8* morphants is not rescued by suppression of *p53* signaling. A, Lateral (first row) and dorsal (second row) bright-field images of wild-type 25-hpf zebrafish noninjected embryos or embryos microinjected (1 nL) with CTRMO (0.6 pmol), MCT8MO (0.8 pmol), or MCT8+p53MO (0.8 + 0.5 pmol). The black box denotes the otic vesicle presented in a higher magnification in the insets. Scale bars, 100 μm. B, Total fluorescence (570 nm) measurement of noninjected and CTRMO, MCT8MO, or MCT8+p53MO microinjected wild-type 25-hpf zebrafish embryos after TUNEL using TMR-red. In the graph in B, bars denote SE, and experimental groups that do not differ significantly bear the same letter ($P > .05$) and those with different letters are significantly different ($P < .0001$) after Bonferroni multiple-comparison test.

mals (Figure 3A). The developing diencephalon, MHB, and hindbrain are most affected in the brain together with the barely perceptible otic capsule in the 25-hpf *mct8* morphant embryos (arrowheads in Figure 3A). Notably, at 25 hpf, the lateral bend at the end of the yolk extension is already evident in the axial trunk (Figure 3A).

Because the *mct8* morphants are smaller, it was hypothesized that this might arise from increased apoptosis, a reported nonspecific effect of some MOs (35). To test this hypothesis, 0.8 pmol MCT8MO and 0.5 pmol p53MO were coinjected (1 nL) to suppress nonspecific p53-mediated apoptosis (35). At 25 hpf, the morphants coinjected with p53 did not differ from embryos microinjected with MCT8MO alone (Figure 3A). To further confirm these observations, whole-body fluorescence was measured in individual embryos from each experimental group (BioTek Synergy HT multimode microplate reader, visible spectrum 570 nm). Fluorescent TMR-Red TUNEL assays revealed similar low levels of apoptosis in noninjected and 0.6-pmol CTRMO microinjected animals, although higher levels were detected in both MCT8MO and MCT8MO+p53 microinjected embryos (Figure 3B). There were no statistical differences in total fluorescence (Figure 3B) between the noninjected and the CTRMO control groups ($P > .05$) or between the MCT8MO and the MCT8MO+p53MO groups ($P > .05$). However, a significant difference was detected between the control groups and the MCT8MO and MCT8MO+p53MO embryos ($P < .0001$). These results were further confirmed by fluorescent microscopy (Supplemental Figure 3). The results indicate that MCT8MO-induced apoptosis is a specific effect caused by lack of maternal TH uptake by the embryo.

To further confirm the specificity of the MCT8MO for the zebrafish wild-type *mct8* mRNA, the first 6 nucleotides in the MO seeding sequence was mutated (*mct8* mRNA) and transcribed in vitro. Microinjection (1 nL) of 100 pg of the mutant *mct8* mRNA did not change zebrafish embryo development over the time period studied (48 hpf). In contrast, 0.8 pmol MCT8MO alone gave rise to the specific phenotype already observed at 48 hpf (Figures 2 and 4A). However, when 0.8 pmol MCT8MO and 100 ng 5′-mutated *mct8* mRNA was coinjected (1 nL), it rescued most of the embryos (62%) (Figure 4, A and B). The coinjected *mct8* mRNA+MCT8MO embryos did not have an axial bend or modified brain development relative to the control embryos (Figure 4A). Because *mct8* is expressed in the neurovasculature by 48 hpf (Figure 1), the development of these structures may give an index of the MCT8MO phenotype. A detailed evaluation of the impact of the MCT8MO on the developing vasculature was revealed using the zebrafish *Tg(fli1:EGFP)* line (Figure 4C). Microinjection of 0.8 pmol MCT8MO disrupted the development of the hindbrain neurovasculature (39, 40) with only 3 of the normal 7 hindbrain-penetrating

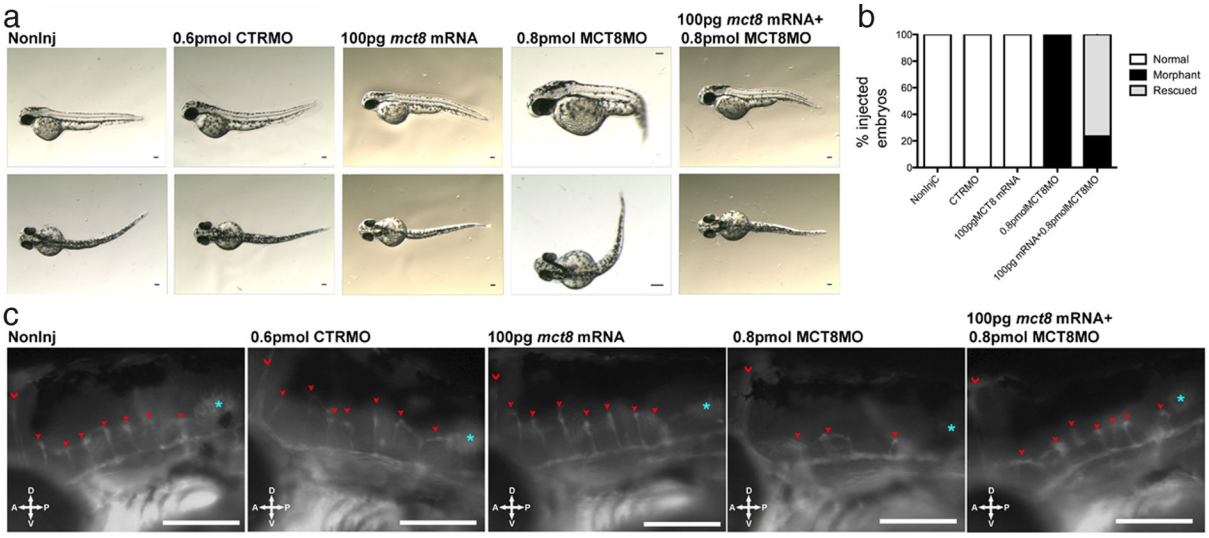

Figure 4. MCT8MO phenotype is rescued by MCT8 mRNA coinjection. A, Lateral (upper row) and dorsal (lower row) bright-field images of *Tg*(*fli1*:*EGFP*) 48-hpf zebrafish embryos noninjected and CTRMO (0.6 pmol), mutated *mct8* mRNA (100 g), MCT8MO (0.8 pmol), or mutated *mct8* mRNA+MCT8MO (100 pg + 0.8 pmol) microinjected (1 nL). Scale bars, 100 μm. B, Distribution of normal, morphant, and rescued animals in the different experimental groups according to axial trunk bending phenotype. C, Fluorescent images of central arteries invading the hindbrain of *Tg*(*fli1*:*EGFP*) 48-hpf zebrafish embryos noninjected and CTRMO, mutated *mct8* mRNA, MCT8MO, or mutated *mct8* mRNA+MCT8MO microinjected. The red chevron denotes midcerebral vein, red arrowheads denote central arteries invading the hindbrain, and cyan asterisk denotes otic capsule. Scale bars, 50 μm.

central arteries being formed (red arrowheads in Figure 4C). Coinjection of both *mct8* mRNA and MCT8MO rescued the embryos, and they resembled the control embryos and developed 7 central arteries in the hindbrain. Overexpression of *mct8* mRNA did not provoke overt modifications in the developing brain vasculature relative to control embryos. Rescue of *mct8* morphants by coinjection of *mct8* mRNA rescued the apoptotic phenotype of maternal TH knockdown (Supplemental Figure 4) and *pax8* expression in the hindbrain (Supplemental Figure 5) and further validated the specificity of the MCT8MO. Rescue of apoptosis by mutated *mct8* mRNA strongly suggests that suppression of apoptosis during zebrafish development is a specific function of the maternal THs (Supplemental Figure 4). Furthermore, rescue of the apoptotic phenotype by restoring MCT8 further confirms the specificity of the MCT8MO and that the phenotype is specific (Supplemental Figure 4). Collectively, the results indicate that MCT8MO is a bona fide knockdown of *mct8* function and consequently maternal TH (20) actions.

Maternal TH knockdown affects brain and spinal cord development

Brain development is significantly perturbed in 25-hpf embryos by MCT8 knockdown (Figure 5A). In control embryos (CTRMO), cells positive for Pax7, which labels several dorsal cell populations in the developing zebrafish brain (41–43), are found in the dorsal midbrain, MHB, hindbrain, and first sections of the spinal cord (red in Figure 5A). In contrast, the *mct8* morphants have a reduced midbrain size and a reduction in pax7-positive cells (Figure 5A). In the MHB and hindbrain, the number of pax7-positive cells is clearly reduced (Figure 5A), and they are undetectable in the first section of the spinal cord (Figure 5B). To further understand the effect of MCT8 knockdown and the role of maternal THs in early brain development, neuron differentiation was assessed with β-tubulin staining (green in Figure 5). Tubulin staining of *mct8* morphants revealed mild effects in the main ventral commissures of the developing brain (Figure 5A). In the hindbrain, *mct8* morphants have fewer tubulin-positive cells than the control embryos (Figure 5A), and this is even more noticeable in the spinal cord (Figure 5C). Compared with the control embryos in the *mct8* morphants, most medial spinal cord neurons (cyan arrowheads in Figure 5C) are almost all absent, and there is an apparent increase in most ventrally located motoneuron-like neurons (green arrowheads in Figure 5C). The number, diversity, and morphology of dorsal spinal cord neurons are also affected in the *mct8* morphants (red arrowheads in Figure 5C), and only a single type of dorsal spinal cord neurons develop (Figure 5C). The cell body of dorsal spinal cord neurons in MCT8 morphants is modified relative to the control because it is perpendicular to the sagittal plane of the embryo and the axons project contralaterally

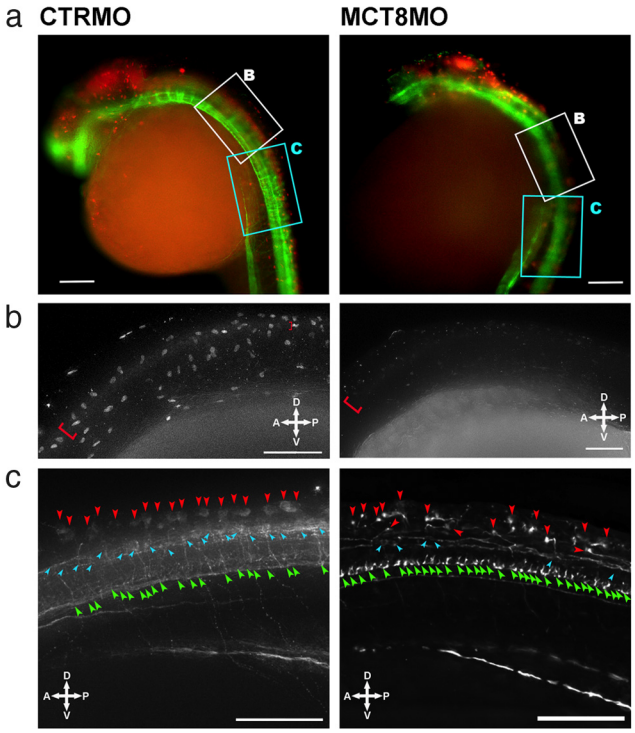

Figure 5. MCT8 knockdown affects brain and spinal cord development. A, Fluorescent images of 25-hpf wild-type zebrafish embryos microinjected with either CTRMO or MCT8MO. Red and green represent, respectively, Pax7 and acetylated β-tubulin immunostaining. The white and cyan boxed area denotes, respectively, the high-magnification images presented in B and C. Scale bars, 100 μm. B, Higher magnification of the most anterior spinal cord section of 25-hpf wild-type zebrafish embryos microinjected with either CTRMO or MCT8MO (white boxed area in A) after immunostaining for Pax7. The red brackets denote Pax7-positive spinal cord cells along the dorsal region of the developing spinal cord. In the MCT8 morphant, only the most anterior dorsal spinal cord has a few Pax7-positive cells. Scale bars, 50 μm. C, Higher magnification of sections 4 to 10 of the spinal cord in 25-hpf wild-type zebrafish embryos microinjected with either CTRMO or MCT8MO (white boxed area in A) after immunostaining for acetylated β-tubulin. Dorsal (red arrowheads), medial (cyan arrowheads), and ventral (green arrowheads) positioned spinal cord neurons are highlighted. Scale bars, 50 μm.

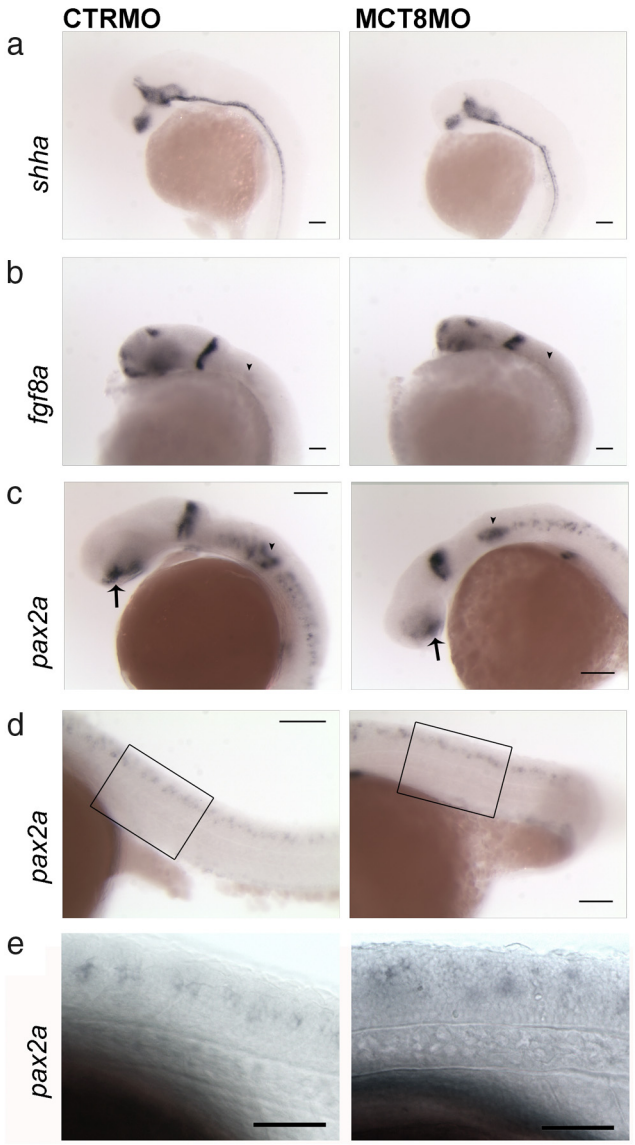

Figure 6. *pax2a* is a target of maternal THs in a context-related fashion. *shha* (A), *fgf8a* (B), and *pax2a* (C, D and, E) WISH expression in 25-hpf wild-type zebrafish embryos microinjected with either CTRMO or MCT8MO. Arrowheads in B denote the otic vesicle expression field of *fgf8*. Arrowheads in C denote otic vesicle expression of *pax2a*, and arrows denote the optic stalk expression field. Boxed areas in D represent the high-magnification images shown in E. Scale bars, 50 μm (A, B, and E) and 100 μm (C and D).

and then bend (90° angle) down toward the ventral floor (red arrowheads in Figure 5C).

To determine where maternal THs act in the genetic cascade of brain and spinal cord development, the expression of *fgf8a*, *shha*, and *pax2a* was analyzed in 25-hpf embryos (Figure 6). The expression of *fgf8a*, *shha*, and *pax2a* in *mct8* morphants is similar to the control embryos (Figure 6A). The *mct8* morphants (25 hpf) are smaller than control embryos and have a corresponding reduction in the expression field of *fgf8a* (Figure 6B), and its expression is disrupted only in the developing otic capsule (arrowheads in Figure 6B). The expression of *pax2a* is also affected in the otic capsule at 25 hpf (arrowheads in Figure 6C), and in *mct8* morphants, it has a widespread expression in the vesicle, whereas in control embryos, the *pax2a* is low intensity in the periphery and higher intensity in the cells that generate the otoliths (arrowheads in Figure 6C). The *mct8* morphant has impaired eye development, and this is associated with a reduction in *pax2a* expression in the anterior region of the developing optic stalk (arrows in Figure 6C). In the MHB, *pax2a* expression is unchanged in *mct8* morphants relative to the control embryos apart from a reduction in the expression field (Figure 6C) that is commensurate with the reduction in the size of their brain (Figure 3A). MCT8 knockdown also affects *pax2a* expression in the hindbrain (Figure 6C), and in the first 3 rhombomeres, no *pax2a*-expressing

cells are detected, which contrasts with the abundant expression in the control embryos (Figure 6C). From rhombomere 4 onward, expression of *pax2a* is detected in the hindbrain of *mct8* morphants, although it has a more random distribution and is scattered dorsoventrally rather than being an almost straight row of cells typical of control embryos (Figure 6C). In the spinal cord of *mct8* morphants, distribution of *pax2a*-expressing cells is random, and they are scattered dorsoventrally relative to the control embryos (Figure 6, D and E).

To establish whether MCT8 knockdown (and removal of maternal THs) affects other neural cell populations, zebrafish development was studied up until 31 hpf when the first hindbrain interneurons start to differentiate. Immunostaining with Zn8 antiserum (neurolin) reveals a significant reduction in the labeling of the trigeminal nerves in the *mct8* morphants (red asterisks in Figure 7A), suggesting a decrease in the number of these neurons. Only a few differentiated hindbrain interneurons are present at 31 hpf in *mct8* morphants, unlike control embryos that have high numbers of these neurons (arrowheads in Figure 7A). Expression of *pax2a* in the hindbrain at 31 hpf in *mct8* morphants is similar to that observed at 25 hpf (Figures 6C and 7B) with the exception of a few *pax2a*-expressing cells in the first 3 rhombomeres (Figure 7B). The expression of *pax2a* in the MHB in *mct8* morphants at 31 hpf is identical to the control embryos when size differences in the MHB are taken into account (Figure 7B). In the otic capsule, expression of *pax2a* is concentrated in a paired group of cells in control embryos, and in the *mct8* morphants, the expression fields are smaller and closer together (arrowheads in Figure 7B). In the spinal cord of 31-hpf MCT8MO morphants, the distribution of *pax2a*-positive cells is similar to that at 25 hpf. The *pax2a*-positive spinal cord neurons are fewer and more dispersed and have a more random distribution along the dorsoventral axis (Figure 7B). Moreover, β-tubulin immunostaining reveals that as observed at 25 hpf (Figure 5C), neurons are fewer and less diverse, and those present have an aberrant distribution and morphology (Figure 7C). In *mct8* morphants at 31 hpf, *pax8* expression is reduced and low expression occurs in the MHB and is absent from the hindbrain, unlike the control embryos (Figure 7D). Because *pax8* is a marker of some hindbrain interneuron's reduction in its expression is unsurprising given the dramatic reduction in the number of these cells in the *mct8* morphants (Figure 7, A and D). The knockdown of *Pax8* expression continues at 48 hpf in both the brain (Figure 2B) and spinal cord of *mct8* morphants relative to the control embryos (Figure 7, E and F) and suggests that *pax8* inhibitory neurons (38) do not differentiate normally in the *mct8* morphants.

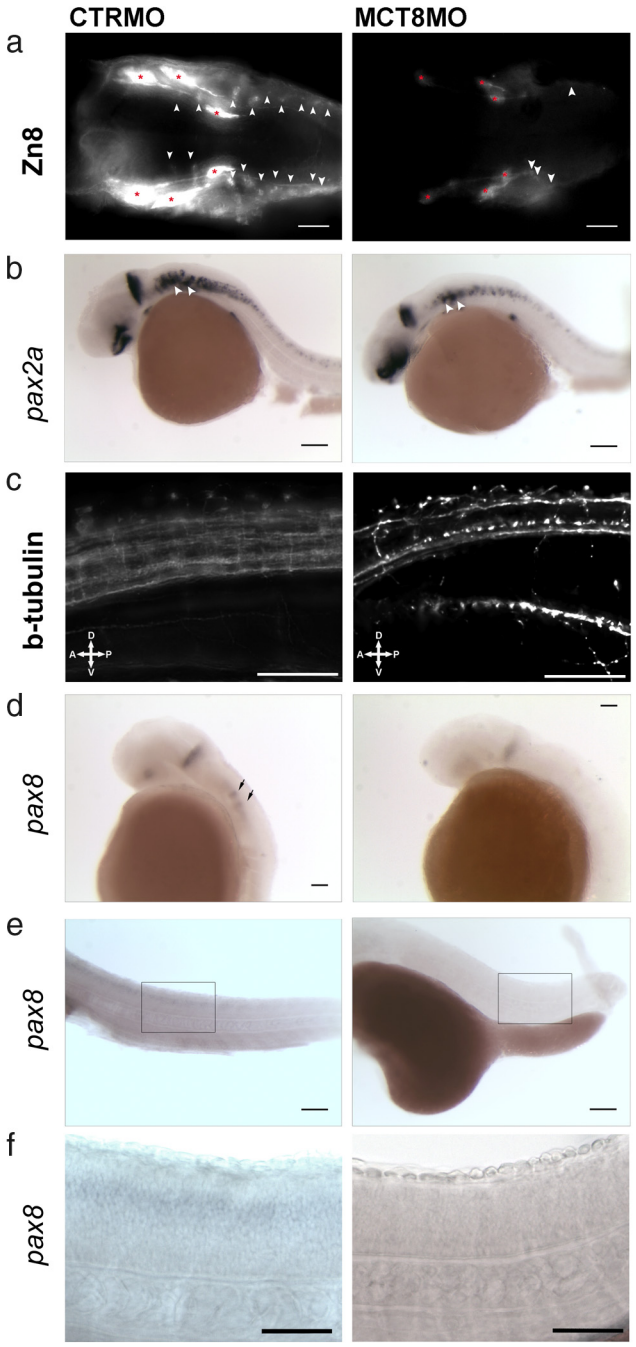

Figure 7. At 31 (A–D) and 48 (E and F) hpf, *mct8* morphants have fewer hindbrain and spinal cord neurons. A, Immunodetection of Zn8 in the hindbrain of 31-hpf wild-type zebrafish embryos microinjected with either CTRMO or MCT8MO. Arrowheads in A denote hindbrain interneurons, and red asterisks indicate trigeminal neurons. Scale bars, 50 μm. B, Expression of *pax2a* in 31-hpf wild-type zebrafish embryos microinjected with either CTRMO or MCT8MO. Black arrowheads indicate otic vesicle expression of *pax2a*. Scale bars, 100 μm. C, Immunodetection of acetylated β-tubulin in segments 4 to 10 of the spinal cord in 31-hpf wild-type zebrafish embryos microinjected with either CTRMO or MCT8MO. Scale bars, 50 μm. D, Expression of *pax8* in 31-hpf wild-type zebrafish embryos microinjected with either CTRMO or MCT8MO. Arrows indicate first *pax8*-positive hindbrain interneurons. Scale bars, 50 μm. (e) Spinal cord expression of *pax8* in 48-hpf wild-type zebrafish embryos microinjected with either CTRMO or MCT8MO. Scale bars, 200 μm. The boxed area in E corresponds to a higher-magnification image in F. Scale bars, 50 μm (F).

Maternal THs are involved in zebrafish locomotor neural network development

To further understand the functional consequence of the lack of maternal THs on the spinal cord neural networks, a touch-and-go mobility assay was employed (Figure 8). Comparison of control animals at 72 hpf and *mct8* morphants with the characteristic bent trunk phenotype revealed that they exhibited severely impaired mobility (Figure 8A and Supplemental Movie 1 and Supplemental Movie 2) ($P < .0001$; Figure 8B). This results show that maternal THs are also important in the establishment of the spinal cord neural networks during zebrafish development.

Discussion

In the present study, knockdown of zebrafish MCT8, the exclusive transporter of THs, revealed that maternal THs have an essential role in zebrafish brain and spinal cord development. The presence of hormones in teleost eggs is well established (22), and zebrafish eggs, like other teleost eggs, are rich in maternal THs (20). In addition, the molecular components for TH cellular action are present in early zebrafish embryos (Figure 1 and Supplemental Figure 1) (24–28, 30). The general view has been "that in zebrafish embryonic development thyroid receptors are not part of TH signaling but are coregulatory factors of retinoic acid signaling" (24, 25), although more recent evidence implicates THs in teleost embryonic development (44). Attempts to establish the action of TH-activated genes in zebrafish embryonic development have as yet been inconclusive and have yielded relatively little insight into the actions of maternal THs on zebrafish development (30, 44–47). Here we demonstrated that THs are bona fide maternally derived signaling molecules essential for normal nervous system development participating in regionalization and differentiation of specific neural cell lineages in the brain and spinal cord of developing zebrafish embryos. Moreover, the study reveals that the modifications in brain development and mobility provoked by MCT8 knockdown during embryogenesis cannot be reversed at 72 hpf when zebrafish larvae start to produce endogenous THs (32) (Figure 8). The results reveal a critical role for maternal THs in normal brain development before hatching and indicate that failures in TH supply during this time lead to irreversible changes. From a comparative perspective, the *mct8* morphant phenotype (impaired locomotor capacity and stiffness of the posterior body) is reminiscent of humans with the X-linked mental retardations that arise due to mutations in the *MCT8* gene (48, 49).

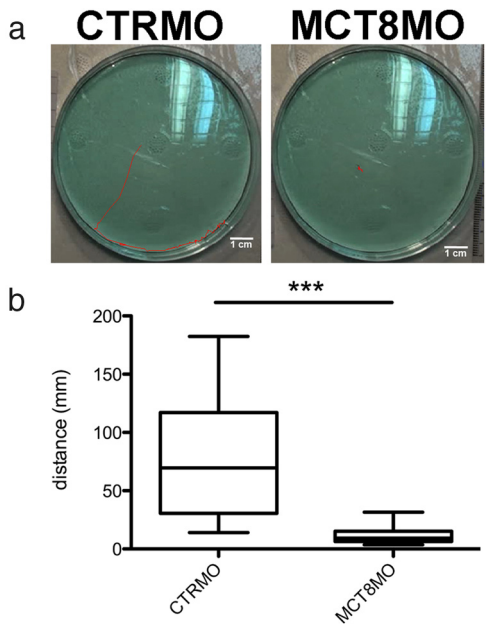

Figure 8. *mct8* morphants have impaired mobility at 72 hpf. A, Typical image depicting the total distance covered in 2 minutes by 72-hpf wild-type zebrafish embryos or embryos microinjected with either CTRMO or MCT8MO. Scale bar, 1 cm. B, Box and whisker graphic (minimum and maximum) of the distance covered in 1 minute after touch of 72-hpf wild-type zebrafish embryos microinjected with either CTRMO or MCT8MO. ***, Significant statistical differences ($P < .0001$) between the experimental groups (Dunnet's multiple-comparison test).

The working hypothesis of the present study was that if maternal THs play a role in zebrafish embryo development, then blocking their access to the embryo should generate a phenotype. It was reasoned that knockdown of the highly specific TH cellular transporter MCT8 would effectively stop uptake of maternal THs by the embryo (29). The expression of *mct8* in zebrafish embryos and its distribution (Figure 1 and Supplemental Figure 1) gave insight into the likely sites of action of maternally derived T_3. Knockdown of MCT8 function via MOs severely affected the brain regions (Figures 2–7) where *mct8*, *thrab*, and to some extent *thraa* are expressed during zebrafish development (Figure 1 and Supplemental Figure 1) (28, 30) and support a role for maternal THs in this process. The phenotype of the *mct8* morphant with the translation-blocking MO is similar to the one found with splicing and 3′-untranslated zebrafish *mct8* MOs (30). Moreover, the effects of the MCT8MO on apoptosis are not suppressed by a p53MO but are reversed by coinjection of a silent-mutated mRNA for zebrafish *mct8*, indicating that the effects are specific (Figure 3 and Supplemental Figure 4). THs are known to be a strong enhancer of cell survival and differentiation during vertebrate development and adult life (9, 10, 16, 50–53). This is also true during zebrafish development when maternal THs contribute to decreased apoptosis of different cell types in the

embryo (Figure 3B). Moreover, when access to maternal THs is interrupted in the *mct8* morphant, apoptosis in 25-hpf zebrafish embryos increases, and the results suggest it may be independent or may act upstream of the *p53* signaling pathway (Figure 3). Rescue of the mct8 morphant apoptosis phenotype by coinjection of a 6-bp mutated (MO mismatch) *mct8* mRNA (Supplemental Figure 4) supports the involvement of maternal THs in survival of specific cell types during zebrafish development. However, the mechanism by which it occurs and the identity of the cells is still unresolved, and more detailed studies are needed. It will be important in the future to assess the effect of maternal THs on proliferation. Nonetheless, the results of our study show very clearly that maternal THs are involved in cell differentiation and survival by suppressing apoptosis in target cells. The analysis carried out does not allow us to infer the mechanisms by which maternal THs regulate cell survival/apoptosis in the zebrafish embryo. Nonetheless, the present p53MO data indicate that p53 signaling is probably not involved in TH-mediated cell survival in the zebrafish embryo. Taken together, the results support the hypothesis that maternal THs are bona fide signaling molecules that participate, via *mct8*, in normal embryonic development of zebrafish.

The phenotype of the MCT8 knockdown recapitulates that obtained when THs are reduced or other elements of the TH cellular signaling cascade are modified during development in other vertebrates (6, 9, 48, 54) or in zebrafish embryonic development (24, 25). The fact that *mct8* morphants and zebrafish embryos overexpressing *thraa* (25) both exhibit severe hindbrain defects (Figures 5–7) indicates that the role of TRs in early embryonic development of zebrafish might not be exclusively to repress retinoic acid signaling but also to regulate gene expression of maternal TH target genes. It was not possible to precisely resolve the mechanisms by which maternal THs modulate zebrafish brain development. However, the absence of change in *shha* and *fgf8a* expression in developing neural tissues of the *mct8* morphants relative to control embryos suggest it is not via regulation of these pathways (Figure 6, B and C), further suggesting that maternal THs are not involved in early specification of neural tissues. However, ablation of *fgf8a* expression in the otic capsule of *mct8* morphants suggests that maternal THs may regulate developmental events upstream of *fgf8a* signaling in a cell-specific manner. In zebrafish, there are no reports about regulation of *fgf8a* or other *fgf* genes by THs; nonetheless, hypothyroidism in mice during postnatal development decreases *Fgf2* expression in the microvasculature of the brain (55). Furthermore, in a mouse model of hypoxia, T_4 treatment upregulated *FGF2* and *FGFR1* in the microvasculature of the lung (56). Observations of *Fgf* gene responsiveness to THs in other vertebrates provides support for the potential role of maternal THs in the developing otic capsule in zebrafish, and further studies using transplantation of zebrafish embryo cells mutant for the *mct8* gene would clarify this issue. Currently, such experiments are not possible because no *mct8* mutant lines are available.

The expression of *pax8*, *pax2a*, and Pax7 in the developing zebrafish brain is substantially modified in the *mct8* morphant (absence of maternal THs) (Figures 2 and 5–7). However, for Pax7 and *pax2a*, the effect is not uniform in all brain regions and occurred in a cell-specific manner (Figures 5 and 6). The lack of effect of MCT8 knockdown on *pax2a* compared with *pax8* expression in the MHB (Figures 6 and 7) suggests that maternal THs are involved in the genetic cascade regulating *pax8* upstream or independently of *pax2a* (57). The number of Pax7-positive cells in the brain and spinal cord as well as the number of xantophores and muscle satellite cells in the axial muscle of *mct8* morphants decreased (Figure 5, A and B), suggesting that maternal TH signaling is required upstream of Pax7 for correct expression but is not essential. This might indicate that maternal TH signaling acts upstream of Pax7 in these cell types. Given the role of Pax7 in dorsal determination of neural progenitor cell identities (41–43, 58), the results suggest that maternal THs may be an important factor for the dorsal determination of different regions of the brain and spinal cord at or even before 25 hpf. *Wnt* signaling expands *pax7* in the preplacodal region (59), whereas *Wnt* antagonists have the opposite action (58, 60). The modification of Pax7 expression in *mct8* morphants is reminiscent of what occurs when *wnt* signaling is disrupted in developing zebrafish brain and suggests that maternal THs could be involved in the regulation of components of the *wnt* signaling cascade in dorsal brain and spinal cord regions. However, more experiments will be required to test this hypothesis. The observation that *pax8* expression is totally suppressed (Figures 2 and 7) and *pax2a* expression is disrupted in the optic stalk, otic capsule, and hindbrain and spinal cord (Figures 6 and 7) in the *mct8* morphants strengthens the notion that maternal THs are involved in specification of different neural cell populations during zebrafish development (38, 57, 59). This observation is reinforced by the substantial decrease in the number of Zn8-positive interneurons in the hindbrain (Figure 7). The way maternal THs regulate *pax2a*, *pax7*, and *pax8* expression in the developing zebrafish brain remains unresolved, but *wnt* signaling is a candidate of interest.

The spinal cord is most affected in the *mct8* morphants. During normal development spinal cord neurons increase in number and diversity along the dorsal-ventral

axis (Figures 5C and 7), but this diversity is lost in *mct8* morphants, suggesting this tissue is an important target for maternal THs (Figures 5–7). The modifications in spinal cord development in the *mct8* morphants coincides with the absence of Pax7-positive cells, which are involved in dorsal spinal cord neuron progenitor differentiation (41–43, 58). Zebrafish *pax8* and *pax2a* are also involved in cell fate determination of spinal cord neurons (38, 61) and have a disrupted expression in the *mct8* morphants. They act independently or in conjunction and generate different spinal cord interneurons with inhibitory characteristics (38, 62). Whereas *pax8* is found only in commissural bifurcating longitudinal neurons (38), *pax2a* is found mostly in glycinergic or GABAergic inhibitory neurons, including the most ventral spinal circumferential ascending interneurons. There is almost total suppression of most ventral ascending neurons in the spinal cord of *mct8* morphants in the regions where *pax2a* and *pax8* are expressed (Figures 5–7). Taken together, the evidence suggests that maternal THs contribute to the specification of different spinal cord populations via regulation of *pax7*, *pax2a*, and *pax8*. Strikingly, not all spinal cord neurons expressing *pax2a* are affected, suggesting that only a small subset of *pax2a*-positive neurons is regulated by maternal THs. Evidence that *pax2a* and *pax8* participate in cell fate decisions in the developing zebrafish spinal cord comes from double mutants for these genes in which commissural bifurcating longitudinal neurons do not differentiate, and instead, their progenitors give rise to neurons with ipsilateral descending axons (38, 61, 63). The higher abundance of the most ventral neurons and decrease in dorsal neurons of the spinal cord in *mct8* morphants suggests that maternal THs might function as a selective signal involved in fate determination of different spinal cord neurons upstream of *pax8*-positive interneurons and also in a small subset of *pax2a*-positive spinal cord neurons. However, more studies will be necessary to fully resolve this question and accurately pinpoint which spinal cord neurons are dependent on maternal THs for normal development. Nonetheless, the overall phenotype of the zebrafish *mct8* morphants, a stiff axial body, with a sharp bend at the end of the yolk extension may be indicative of constant contraction of the axial muscles due to lack of inhibitory spinal cord interneurons and increase in motoneurons. Support for this hypothesis come from observations in mice, *Xenopus*, and zebrafish that *pax2*-positive spinal cord interneurons are involved in the regulation of locomotor activity (63–65) and the reduced mobility exhibited by the zebrafish *mct8* morphants (Figure 8 and Supplemental Movies 1 and 2).

In conclusion, an in vivo assay has been established in the zebrafish for analyzing the function of maternally derived THs in zebrafish eggs. Attempts to directly ablate THs in the egg were not technically possible. This is a limitation of the present study, but given the exclusive function of MCT8 as a TH transporter (29), the MCT8 knockdown phenotype is entirely a result of the absence of TH transport into cells. Nonetheless, using MCT8 knockdown, it is demonstrated that maternal THs are bona fide signaling molecules from as early as, or before, 25 hpf in zebrafish embryonic development. It is revealed that maternal THs are involved in both regional specification of the dorsal roof of the brain and spinal cord but also in cell-specific fate determination of neurons in the hindbrain and spinal cord. Moreover, maternal THs act downstream of *shha* and *fgf8a* signaling but upstream of *pax2a*, *pax7*, and *pax8*. More studies are now required to dissect in detail the maternal TH genetic cascade during zebrafish development. This is the first vertebrate model of embryonic development in which the cellular and molecular consequences of MCT8 knockdown, responsible for X-linked mental retardation in humans (48, 49), are revealed and opens the door for future studies aimed at improving understanding of this human condition.

Acknowledgments

We thank Dr Lisa Maves (*fgf8a*), Dr Sachiko Takayama (*thraa* and *thrab*), and Dr Fumihito Ono (*pax2a*) for the zebrafish plasmids.

Address all correspondence and requests for reprints to: Marco António Campinho, Comparative Endocrinology and Integrative Biology Group, Centre of Marine Sciences, Universidade do Algarve, Campus de Gambelas, Edificio 7, Lab 2.28, 8005–139 Faro, Portugal. E-mail: macampinho@ualg.pt.

This work was funded by the Portuguese Science Foundation (FCT) project PTDC/MAR/115005/2009. M.A.C. is funded by FCT Postdoctoral Grant SFRH/BPD/66808/2009, and J.S. is funded by FCT Postdoctoral Grant SFRH/BPD/67008/2009. C.F. is supported by FCT Project Pest-OE/EQB/LA0023/2013.

Disclosure Summary: All authors have no financial or any other conflict of interest to disclose.

References

1. **Dumitrescu AM, Liao XH, Weiss RE, Millen K, Refetoff S.** Tissue-specific thyroid hormone deprivation and excess in monocarboxylate transporter (Mct) 8-deficient mice. *Endocrinology*. 2006; 147(9):4036–4043.
2. **Wirth EK, Roth S, Blechschmidt C, et al.** Neuronal 3′,3,5-triiodothyronine (T_3) uptake and behavioral phenotype of mice deficient in Mct8, the neuronal T_3 transporter mutated in Allan-Herndon-Dudley syndrome. *J Neurosci*. 2009;29(30):9439–9449.

3. **Ceballos A, Belinchon MM, Sanchez-Mendoza E, et al.** Importance of monocarboxylate transporter 8 for the blood-brain barrier-dependent availability of 3,5,3′-triiodo-L-thyronine. *Endocrinology*. 2009;150(5):2491–2496.
4. **Morte B, Ceballos A, Diez D, et al.** Thyroid hormone-regulated mouse cerebral cortex genes are differentially dependent on the source of the hormone: a study in monocarboxylate transporter-8- and deiodinase-2-deficient mice. *Endocrinology*. 2010:151(5): 2381–2387.
5. **Horn S, Heuer H.** Thyroid hormone action during brain development: More questions than answers. *Mol Cell Endocrinol*. 2010; 315(1–2):19–26.
6. **Braun D, Kinne A, Bräuer AU, Sapin R, et al.** Developmental and cell type-specific expression of thyroid hormone transporters in the mouse brain and in primary brain cells. *Glia*. 2011;59(3):463–471.
7. **Visser WE, Friesema EC, Visser TJ.** Thyroid hormone transporters: the knowns and the unknowns. *Mol Endocrinol*. 2011;25(1):1–14.
8. **Darras VM, Van Herck SL, Geysens S, Reyns GE.** Involvement of thyroid hormones in chicken embryonic brain development. *Gen Comp Endocrinol*. 2009;163:58–62.
9. **Fauquier T, Romero E, Picou F, et al.** Severe impairment of cerebellum development in mice expressing a dominant-negative mutation inactivating thyroid hormone receptor alpha1 isoform. *Dev Biol*. 2011;356(2):350–358.
10. **Wallis K, Dudazy S, van Hogerlinden M,** *Nordström* K, Mittag J, *Vennström* B. The thyroid hormone receptor alpha1 protein is expressed in embryonic postmitotic neurons and persists in most adult neurons. *Mol Endocrinol*. 2010;24(10):1904–1916.
11. **Quignodon L, Grijota-Martinez C, Compe E, et al.** A combined approach identifies a limited number of new thyroid hormone target genes in post-natal mouse cerebellum. *J Mol Endocrinol*. 2007; 39(1):17–28.
12. **Quignodon L, Legrand C, Allioli N, et al.** Thyroid hormone signaling is highly heterogeneous during pre- and postnatal brain development. *J Mol Endocrinol*. 2004; 33(2):467–476.
13. **Hernandez A, Quignodon L, Martinez ME, Flamant F, St. Germain DL.** Type 3 deiodinase deficiency causes spatial and temporal alterations in brain T_3 signaling that are dissociated from serum thyroid hormone levels. *Endocrinology*. 2010;151(11):5550–5558.
14. **Chatonnet F, Picou F, Fauquier T, Flamant F.** Thyroid hormone action in cerebellum and cerebral cortex development. *J Thyroid Res*. 2011;2011:145762.
15. **Darras VM, van der Geyten S, Kuehn ER.** Thyroid hormone metabolism in poultry. *Biotechnol Agron Soc Environ*. 2000;4:13–20.
16. **Zoeller RT.** New insights into thyroid hormone action in the developing brain: the importance of T_3 degradation. *Endocrinology*. 2010;151(11):5089–5091.
17. **Kress E, Samarut J, Plateroti M.** Thyroid hormones and the control of cell proliferation or cell differentiation: Paradox or duality? *Mol Cell Endocrinol*. 2009;313(1–2):36–49.
18. **Dong H, Yauk CL, Rowan-Carroll A, et al.** Identification of thyroid hormone receptor binding sites and target genes using ChIP-on-Chip in developing mouse cerebellum. *PLoS One*. 2009;4(2): e4610.
19. **Dowling AL, Martz GU, Leonard JL, Zoeller RT.** Acute changes in maternal thyroid hormone induce rapid and transient changes in gene expression in fetal rat brain. *J Neurosci*. 2000;20(6):2255–2265.
20. **Chang J, Wang M, Gui W, Zhao Y, Yu L, Zhu G.** Changes in thyroid hormone levels during zebrafish development. *Zool Sci*. 2012;29(3):181–184.
21. **Campinho MA, Galay-Burgos M, Sweeney GE, Power DM.** Coordination of deiodinase and thyroid hormone receptor expression during the larval to juvenile transition in sea bream (*Sparus aurata*, Linnaeus). *Gen Comp Endocrinol*. 2010;165(2):181–194.
22. **Power DM, Llewellyn L, Faustino M, et al.** Thyroid hormones in growth and development of fish. *Comp Biochem Physiol C Toxicol Pharmacol*. 2001;130(4):447–459.
23. **Llewellyn L, Ramsurn VP, Sweeney GE, Wigham T, Power DM.** Expression of thyroid hormone receptor during early development of the sea bream (*Sparus aurata*). *Ann N Y Acad Sci*. 1998;839: 610–611.
24. **Essner JJ, Breuer JJ, Essner RD, Fahrenkrug SC, Hackett PB.** The zebrafish thyroid hormone receptor alpha 1 is expressed during early embryogenesis and can function in transcriptional repression. *Differentiation*. 1997;62(3):107–117.
25. **Essner JJ, Johnson RG, Hackett PB.** Overexpression of thyroid hormone receptor alpha 1 during zebrafish embryogenesis disrupts hindbrain patterning and implicates retinoic acid receptors in the control of hox gene expression. *Differentiation*. 1999;65(1):1–11.
26. **Liu YW, Chan WK.** Thyroid hormones are important for embryonic to larval transitory phase in zebrafish. *Differentiation*. 2002; 70(1):36–45.
27. **Liu YW, Lo LJ, Chan WK.** Temporal expression and T_3 induction of thyroid hormone receptors α1 and β1 during early embryonic and larval development in zebrafish, *Danio rerio*. *Mol Cell Endocrinol*. 2000;159(1–2):187–195.
28. **Bertrand S, Thisse B, Tavares R, et al.** Unexpected novel relational links uncovered by extensive developmental profiling of nuclear receptor expression. *PLoS Genet*. 2007;3(11):e188.
29. **Arjona FJ, de Vrieze E, Visser TJ, Flik G, Klaren PH.** Identification and Functional Characterization of Zebrafish Solute Carrier Slc16a2 (Mct8) as a Thyroid Hormone Membrane Transporter. *Endocrinology*. 2011;152:5065–5073.
30. **Vatine GD, Zada D, Lerer-Goldshtein T, et al.** Zebrafish as a model for monocarboxyl transporter 8-deficiency. *J Biol Chem*. 2013; 288(1):169–180.
31. **Elsalini OA, von Gartzen J, Cramer M, Rohr KB.** Zebrafish hhex, nk2.1a, and pax2.1 regulate thyroid growth and differentiation downstream of Nodal-dependent transcription factors. *Dev Biol*. 2003;263(1):67–80.
32. **Opitz R, Maquet E, Huisken J, et al.** Transgenic zebrafish illuminate the dynamics of thyroid morphogenesis and its relationship to cardiovascular development. *Dev Biol*. 2012;372(2):203–216.
33. **Kimmel CB, Ballard WW, Kimmel SR, Ullmann B, Schilling TF.** Stages of embryonic development of the zebrafish. *Dev Dynam*. 1995;203(3):253–310.
34. **Campinho MA, Power DM.** Waterborne exposure of zebrafish embryos to micromole concentrations of ioxynil and diethylstilbestrol disrupts thyrocyte development. *Aquat Toxicol*. 2013;140–141: 279–287.
35. **Robu ME, Larson JD, Nasevicius A, et al.** p53 Activation by Knockdown Technologies. *PLoS Genet*. 2007;3(5):e78.
36. **Lawson ND, Weinstein BM.** In vivo imaging of embryonic vascular development using transgenic zebrafish. *Dev Biol*. 2002;248(2): 307–318.
37. **Brown D.** *Tracker Video Analysis and Modeling Tool* [computer program]. 2013.
38. **Ikenaga T, Urban JM, Gebhart N, Hatta K, Kawakami K, Ono F.** Formation of the spinal network in zebrafish determined by domain-specific pax genes. *J Comp Neurol*. 2011;519(8):1562–1579.
39. **Isogai S, Horiguchi M, Weinstein BM.** The vascular anatomy of the developing zebrafish: an atlas of embryonic and early larval development. *Dev Biol*. 2001;230(2):278–301.
40. **Ulrich F, Ma LH, Baker RG, Torres-*Vázquez* J.** Neurovascular development in the embryonic zebrafish hindbrain. *Dev Biol*. 2011; 357(1):134–151.
41. **Kawakami A, Kimura-Kawakami M, Nomura T, Fujisawa H.** Distributions of PAX6 and PAX7 proteins suggest their involvement in both early and late phases of chick brain development. *Mech Dev*. 1997;66:119–130.
42. **Lacosta AM, Canudas J, Gonzalez C, Muniesa P, Sarasa M, Dominguez L.** Pax7 identifies neural crest, chromatophore lineages and

pigment stem cells during zebrafish development. *Int J Dev Biol*. 2007;51(4):327–331.
43. **White RB, Ziman MR.** Genome-wide discovery of Pax7 target genes during development. *Physiol Genomics*. 2008;33(1):41–49.
44. **Bohnsack BL, Kahana A.** Thyroid hormone and retinoic acid interact to regulate zebrafish craniofacial neural crest development. *Dev Biol*. 2013;373(2):300–309.
45. **Walpita CN, Crawford AD, Darras VM.** Combined antisense knockdown of type 1 and type 2 iodothyronine deiodinases disrupts embryonic development in zebrafish (*Danio rerio*). *Gen Comp Endocrinol*. 2010;166(1):134–141.
46. **Walpita CN, Crawford AD, Janssens ED, Van der Geyten S, Darras VM.** Type 2 iodothyronine deiodinase is essential for thyroid hormone-dependent embryonic development and pigmentation in zebrafish. *Endocrinology*. 2009;150(1):530–539.
47. **Walpita CN, Van der Geyten S, Rurangwa E, Darras VM.** The effect of 3,5,3′-triiodothyronine supplementation on zebrafish (*Danio rerio*) embryonic development and expression of iodothyronine deiodinases and thyroid hormone receptors. *Gen Comp Endocrinol*. 2007;152(2–3):206–214.
48. **Friesema EC, Visser WE, Visser TJ.** Genetics and phenomics of thyroid hormone transport by MCT8. *Mol Cell Endocrinol*. 2010; 322(1–2):107–113.
49. **Friesema EC, Grueters A, Biebermann H, et al.** Association between mutations in a thyroid hormone transporter and severe X-linked psychomotor retardation. *Lancet*. 2004;364(9443):1435–1437.
50. **Morte B, Manzano J, Scanlan TS, Vennstrom B, Bernal J.** Aberrant maturation of astrocytes in thyroid hormone receptor alpha 1 knockout mice reveals an interplay between thyroid hormone receptor isoforms. *Endocrinology*. 2004;145(3):1386–1391.
51. **Ledda-Columbano GM, Perra A, Pibiri M, Molotzu F, Columbano A.** Induction of pancreatic acinar cell proliferation by thyroid hormone. *J Endocrinol*. 2005;185(3):393–399.
52. **Malo MS, Zhang W, Alkhoury F, et al.** Thyroid hormone positively regulates the enterocyte differentiation marker intestinal alkaline phosphatase gene via an atypical response element. *Mol Endocrinol*. 2004;18(8):1941–1962.
53. **Ledda-Columbano GM, Molotzu F, Pibiri M, Cossu C, Perra A, Columbano A.** Thyroid hormone induces cyclin D1 nuclear translocation and DNA synthesis in adult rat cardiomyocytes. *FASEB J*. 2006;20(1):87–94.
54. **van der Deure WM, Peeters RP, Visser TJ.** Molecular aspects of thyroid hormone transporters, including MCT8, MCT10, and OATPs, and the effects of genetic variation in these transporters. *J Mol Endocrinol*. 2010;44(1):1–11.
55. **Zhang L, Cooper-Kuhn CM, Nannmark U, Blomgren K, Kuhn HG.** Stimulatory effects of thyroid hormone on brain angiogenesis in vivo and in vitro. *J Cereb Blood Flow Metab*. 2010;30(2):323–335.
56. **Al Husseini A, Bagnato G, Farkas L, et al.** Thyroid hormone is highly permissive in angioproliferative pulmonary hypertension in rats. *Eur Respir J*. 2013;41(1):104–114.
57. **Pfeffer PL, Gerster T, Lun K, Brand M, Busslinger M.** Characterization of three novel members of the zebrafish Pax2/5/8 family: dependency of Pax5 and Pax8 expression on the Pax2.1 (noi) function. *Development*. 1998;125(16):3063–3074.
58. **Miyake A, Nihno S, Murakoshi Y, Satsuka A, Nakayama Y, Itoh N.** Neucrin, a novel secreted antagonist of canonical Wnt signaling, plays roles in developing neural tissues in zebrafish. *Mech Dev*. 2012;128:577–590.
59. **Grocott T, Tambalo M, Streit A.** The peripheral sensory nervous system in the vertebrate head: a gene regulatory perspective. *Dev Biol*. 2012;370(1):3–23.
60. **Litsiou A, Hanson S, Streit A.** A balance of FGF, BMP and WNT signalling positions the future placode territory in the head. *Development*. 2005;132(18):4051–4062.
61. **Batista MF, Lewis KE.** Pax2/8 act redundantly to specify glycinergic and GABAergic fates of multiple spinal interneurons. *Dev Biol*. 2008;323(1):88–97.
62. **Satou C, Kimura Y, Higashijima S.** Generation of multiple classes of V0 neurons in zebrafish spinal cord: progenitor heterogeneity and temporal control of neuronal diversity. *J Neurosci*. 2012;32(5): 1771–1783.
63. **Higashijima S, Masino MA, Mandel G, Fetcho JR.** Engrailed-1 expression marks a primitive class of inhibitory spinal interneuron. *J Neurosci*. 2004;24(25):5827–5839.
64. **Gosgnach S, Lanuza GM, Butt SJ, et al.** V1 spinal neurons regulate the speed of vertebrate locomotor outputs. *Nature*. 2006; 440(7081):215–219.
65. **Li WC, Higashijima S, Parry DM, Roberts A, Soffe SR.** Primitive roles for inhibitory interneurons in developing frog spinal cord. *J Neurosci*. 2004;24(25):5840–5848.